

Binding of *lac* repressor-GFP fusion protein to *lac* operator sites inserted in the tobacco chloroplast genome examined by chromatin immunoprecipitation

Christine A. Newell and John C. Gray*

Department of Plant Sciences, University of Cambridge, Downing Street, Cambridge CB2 3EA, UK

Received January 19, 2010; Revised April 29, 2010; Accepted May 4, 2010

ABSTRACT

Chromatin immunoprecipitation (ChIP) has been used to detect binding of DNA-binding proteins to sites in nuclear and mitochondrial genomes. Here, we describe a method for detecting protein-binding sites on chloroplast DNA, using modifications to the nuclear ChIP procedures. The method was developed using the *lac* operator (*lacO*)/*lac* repressor (LacI) system from *Escherichia coli*. The *lacO* sequences were integrated into a single site between the *rbcL* and *accD* genes in tobacco plastid DNA and homoplasmic transplastomic plants were crossed with transgenic tobacco plants expressing a nuclear-encoded plastid-targeted GFP-LacI fusion protein. In the progeny, the GFP-LacI fusion protein could be visualized in living tissues using confocal microscopy, and was found to co-localize with plastid nucleoids. Isolated chloroplasts from the *lacO*/GFP-LacI plants were lysed, treated with micrococcal nuclease to digest the DNA to fragments of ~600 bp and incubated with antibodies to GFP and protein A-Sepharose. PCR analysis on DNA extracted from the immunoprecipitate demonstrated IPTG (isopropylthiogalactoside)-sensitive binding of GFP-LacI to *lacO*. Binding of GFP-LacI to endogenous sites in plastid DNA showing sequence similarity to *lacO* was also detected, but required reversible cross-linking with formaldehyde. This may provide a general method for the detection of binding sites on plastid DNA for specific proteins.

INTRODUCTION

Chromatin immunoprecipitation (ChIP) has been widely used as a means of identifying regions of DNA interacting with specific proteins in nuclei of many organisms (1–5). ChIP has also been used to examine interactions of proteins with mitochondrial DNA in yeast and in a human cell line (6–8). So far there has been only one report of the use of ChIP to investigate protein–DNA interactions in chloroplasts (9), but the WHY1 protein under investigation bound to all regions of maize chloroplast DNA and sequence-specific protein-binding sites were not detected (9). Several specific protein–DNA interactions in chloroplasts have been described (10–17), but these interactions have either been based on experiments *in vitro*, using footprinting (10,11), electrophoretic mobility shift assays (10,11,13) or South-western blotting (12) or on functional effects of gene knockouts or silencing the expression of genes encoding DNA-binding proteins *in vivo* (15–17).

We have attempted to develop a generic method for investigating protein–DNA interactions in chloroplasts, based on the protocols developed for ChIP with nuclear and mitochondrial genes. Unfortunately, none of the specific DNA–protein interaction systems so far described for chloroplasts seemed sufficiently robust to form the basis for developing a ChIP protocol, because of insufficient knowledge of the affinity of the protein for the binding site. It was decided to introduce a very well-characterized DNA–protein interaction system, the *lac* operator (*lacO*)/*lac* repressor (LacI) system from *Escherichia coli* (18), into tobacco chloroplasts to provide plant material for the development of a ChIP protocol. The *lacO*/LacI system has previously been shown to provide IPTG-inducible regulation of gene expression in tobacco chloroplasts (19).

*To whom correspondence should be addressed. Tel: +44 1223 333925; Fax: +44 1223 333953; Email: jcg2@cam.ac.uk

An advantage of the *lacO*/LacI system is the ability of GFP-tagged fusion proteins of LacI to bind to *lacO* sites in a variety of organisms *in vivo*. In Chinese hamster ovary and yeast cells, a GFP-LacI fusion protein has been employed to detect tandem *lacO* sequences inserted at various places around the genome thereby enabling observations of operator-tagged chromosomal DNA *in vivo* (20,21). In *E. coli*, the technique has allowed investigations of DNA segregation (22). In higher plants, Kato and Lam (23) used *lacO*/GFP-LacI to tag chromosomes in transgenic *Arabidopsis thaliana* and thus enable visualization of genomic loci, nucleolar locations and chromatin organization. Similarly Matzke *et al.* (24) reported the successful tagging of transgenic loci in *A. thaliana* with *lacO* and a GFP-LacI fusion protein and subsequent observation of fluorescent spots in interphase nuclei of various cell types. The use of GFP-tagged LacI in chloroplasts should provide additional visual evidence for its interaction with plastid DNA *in vivo*.

Plastid DNA appears as tightly coiled particulate structures, known as nucleoids (25), which are composed of DNA-binding proteins, plastid DNA and uncharacterized RNA (26). Nucleoids can be visualized by fluorescence microscopy after staining with a DNA-specific fluorochrome, such as 4',6-diamidino-2-phenylindole (DAPI; 27). Plastid nucleoids have also been visualized by fusing GFP to the plastid envelope DNA-binding (PEND) protein (28), providing a major advantage over DAPI in that plastid DNA can be located in living, intact tissues, including non-chlorophyll-containing tissues such as roots and flowers. This article describes the development of a ChIP protocol for the detection of GFP-LacI binding to *lacO* and related sequences in tobacco chloroplasts. It may provide a generic method for examining protein–DNA interactions in chloroplasts.

MATERIALS AND METHODS

Plant material

Plants of *Nicotiana tabacum* cv ‘Petite Havana’ and experimental lines used for DNA immunoprecipitation were grown axenically as described in Birch-Machin *et al.* (29). Plants were grown under 16-h light/8-h dark at 23°C with light intensity of 50 $\mu\text{mol m}^{-2} \text{s}^{-1}$. Young leaves ~2.5-cm long from 8–12-week-old plants of Petite Havana were used for particle bombardment while similar-sized leaves from *lacO*, GFP-LacI, *lacO*/GFP-LacI and *Prrn::gfp* lines were used for DNA immunoprecipitation. Fully expanded 5-cm leaves of Petite Havana from axenically grown plants maintained by monthly subculture were used for nuclear transformation. Experimental lines used for crosses and seed production were grown to maturity in a greenhouse with supplementary lighting from 400-W high-pressure sodium lamps (TRS400L Grolox 40; <http://www.sylvania.com>) to give a 16-h day length at a temperature of 23°C.

Gene constructs

Constructs for plastid transformation containing *lacO* repeats were produced in pZS-JH1, a derivative of

pZS197 (30) containing a polylinker in the unique Bsu36I site (31). A plasmid containing the chimeric gene construct *PpsbA-gfp* in pZS-JH1 (31) was digested with HindIII and SmaI to remove *PpsbA-gfp*. *lacO* repeat sequences of 1 or ~2.5 kb were excised from plasmids pAFS52 or pAFS59 (21) by restriction digestion with HindIII and SmaI, and ligated into the corresponding restriction sites of digested pZS-JH1.

Constructs encoding chloroplast-targeted protein fusions of LacI and GFP were assembled in pUC18 and transferred to pBIN19 (32) for nuclear transformation. For the *gfp-lacI* construct, the *lacI* coding sequence (33) was PCR-amplified from *E. coli* XL1-Blue (Stratagene, <http://www.stratagene.com>) using forward (5'-ACGGGA TCCGTGAAACCAGTAACGTTATACGATGTC) and reverse (5'-TTATAAGAGCTCTCACTGCCCGCTTTC CAGTCGGG) primers, introducing a stop codon and inserting BamHI and SacI restriction sites (underlined) at the 5'- and 3'-ends, respectively. The *gfp* coding region was excised from pUCRbcSTP-*gfp* containing the *CaMV* 35S promoter, a region encoding the pea Rubisco small subunit transit peptide (*RbcSTP*), *gfp* and *nos* terminator, by digestion with BamHI and SacI. The amplified fragment containing the *lacI* coding region was then inserted between the BamHI and SacI sites in digested pUCRbcSTP-*gfp* to produce pUCRbcSTP-*lacI*. The *gfp* coding region was amplified from pUCRbcSTP-*gfp* using forward (5'-TGATCTAGACCTAAAGGAGAAGA ACT TTTC) and reverse (5'-ATATGGATCCTTTGTATAGT TCATCCATGCC) primers resulting in the removal of the stop codon and introduction of XbaI and BamHI restriction sites (underlined) at the 5'- and 3'-ends, respectively. This fragment was inserted into XbaI and BamHI-digested pUCRbcSTP-*lacI* directly upstream of *lacI* to produce pUCRbcSTP-*gfp-lacI*.

For the *lacI::gfp* construct, the *lacI* coding sequence was PCR amplified from *E. coli* XL1-Blue using forward (5'-AGTCTAGAGTGAAACCAGTAACGTTATACGA TGTC) and reverse (5'-TTATTTAGGCCTCTGCCCGC TTTCCAGTCGGGAAAC) primers, omitting the *lacI* stop codon and introducing XbaI and StuI sites (underlined) at the 5'- and 3'-ends, respectively. The amplified fragment was inserted into XbaI and StuI sites located directly upstream of *gfp* in pUCRbcSTP-*gfp*, to produce pUCRbcSTP-*lacI-gfp*.

The two chimeric gene-fusion constructs in pUC18, consisting of the *CaMV* 35S promoter, regions encoding the RbcS transit peptide and the GFP fusion protein, and the *nos* terminator, were removed by digestion with HindIII and EcoRI and ligated into the HindIII and EcoRI sites of pBIN19 (32). The constructs in pBIN19 were then introduced into *Agrobacterium tumefaciens* strain LBA4404 (34) by electroporation (35).

Plant transformation

Plastid transformation of tobacco with plasmids containing 1 or ~2.5 kb of *lacO* sequence was carried out by particle bombardment as described by Birch-Machin *et al.* (29). Nuclear transformation of tobacco with *A. tumefaciens* strain LBA4404 containing either *gfp-lacI*

or *lacI-gfp* was accomplished by the leaf disk method, as described by Horsch *et al.* (36), using kanamycin for selection. Regenerated lines were assessed for GFP expression by confocal microscopy. Plastid transformants containing *lacO* were used as female parents in crosses with *gfp-lacI* nuclear transformants in order to combine *lacO* and *gfp-lacI*; expression of GFP was confirmed by confocal microscopy.

Microscopy

Chloroplasts were viewed by laser scanning confocal microscopy (Leica TCS-NT, DMRXA light microscope stand, Leica Microsystems Wetzlar GmbH, <http://www.leica.com>). GFP and chlorophyll fluorescence, following excitation at 488 nm, were collected through TRITC and FITC filters, respectively. Leaf tissue stained with DAPI (1 µg/ml) was observed with a Nikon Optiphot-2 microscope adapted for epifluorescence, using filters XF06 and XF76 (Omega Optical Inc., <http://www.omegafilters.com>) for DAPI and GFP fluorescence, respectively.

Southern blot and PCR analysis of *lacO* transplastomic plants

Total DNA was isolated from young leaves of wild-type and transplastomic tobacco plants using a ChargeSwitch gDNA Plant Kit (Invitrogen; <http://www.invitrogen.com>) and analysed by Southern blotting as described previously (29). Total leaf DNA (0.3 µg) was cut with EcoRV and SacII and fractionated by electrophoresis in a 1% agarose gel; DNA was blotted onto GeneScreen Plus nylon membrane (<http://www.perkinelmer.com>) and probed with a ³²P-labelled 1.24 kb BamHI fragment from *rbcL*, as described previously (29). Total leaf DNA of wild-type and transplastomic *lacO* plants was analysed by PCR in a 25 µl reaction volume containing 0.5-µl DNA template, 0.5 u KOD Hot Start DNA polymerase (Novagen, <http://www.emdbiosciences.com>), 2.5 µl of 10× reaction buffer supplied with the enzyme, 1 mM MgSO₄, 200 µM each of dATP, dCTP, dGTP, dTTP and 0.3 µM of each primer. The PCR programme was as follows: 94°C (2 min), 30 cycles of 94°C (30 s), 55°C (1 min), 72°C (2 min) and 72°C (10 min). PCR fragments were resolved by electrophoresis on a 1% agarose gel containing 0.2 µg ethidium bromide ml⁻¹ and visualized with an AlphaImager 1200 (AlphaInnotech Corp., <http://www.alphainnotech.com>). Primers used to confirm the presence of *lacO* included a forward primer at the 3'-terminal end of *rbcL* (5'-TTGACTAAGTATATACTACCTAG) and a reverse primer in the *accD* flanking region (5'-TTCAGGGAACTACAACTACAGG).

Chloroplast DNA immunoprecipitation

Chloroplast DNA-protein complexes were isolated from young leaves of tobacco as follows. Leaf tissue (2.5 g) was homogenized in 50 ml ice-cold sucrose isolation medium [SIM; 0.35 M sucrose, 25 mM HEPES-NaOH pH 7.6, 2 mM EDTA, 2 mM L-ascorbic acid, 1 mM phenylmethylsulphonyl fluoride (PMSF), 1 mM benzamidine, 5 mM 6-aminocaproic acid, 0.1% BSA], using a Polytron PT3100 fitted with homogenizer PT-DA 3020/2MEC/KL

(Kinematica AG, <http://www.kinematica.ch>) for 30 s at speed 8. The resulting suspension was filtered through eight layers of muslin into a 50 ml centrifuge tube and centrifuged at 1600g for 5 min at 4°C. The pellet was re-suspended in 20 ml SIM and recentrifuged. The washed pellet was resuspended in 1 ml suspension buffer (1 ml SIM to which was added 2.5 mM DTT, 0.5 mM PMSF, 0.5 µg antipain ml⁻¹, 0.5 µg leupeptin ml⁻¹). If a formaldehyde cross-linking step was included, cross-linking of proteins to DNA was carried out by adding 28 µl of 37% formaldehyde to 1 ml chloroplast suspension followed by incubation at 22°C for 10 min. Glycine (150 µl of 1M) was added to remove excess formaldehyde and the suspension incubated for a further 5 min. Chloroplasts were pelleted at 5900g in a microcentrifuge for 5 min at 4°C and the pellet resuspended in 0.5 ml lysis buffer (2% Nonidet P-40, 50 mM Tris-HCl pH 7.6, 1.2 mM spermidine, 1 mM PMSF, 0.1 µg antipain ml⁻¹, 0.1 µg leupeptin ml⁻¹). At this stage, the DNA was sheared either by sonication or by micrococcal DNase digestion. In the early stages of development of the method, the suspension was subjected to sonication with an MSE Soniprep 150 (Sanyo-Gallenkamp, <http://www.sanyogallenkamp.com>), incubating the suspension on ice and keeping the sonication times to short bursts of 10 s at 18–20 µm amplitude and allowing the suspension to rest on ice for 5 min between each sonication. For micrococcal DNase digestion, 125 µl of 50 mM Tris-HCl pH 7.6, 5 mM MgCl₂ and 125 µl of 6× nuclease digestion buffer (90 mM NaCl, 24 mM CaCl₂) were added to 500 µl of lysed chloroplasts. Micrococcal DNase (0.03 units) (micrococcal nuclease from *Staphylococcus aureus*; Sigma-Aldrich, <http://www.sigmaaldrich.com>) was added to the tube and the suspension was incubated at 37°C. After 10 min, 62 µl of 0.5 M EGTA was added to stop nuclease activity and the tube was incubated 5 min on ice. The sample was centrifuged at 5900g for 10 min at 4°C and 0.8 ml supernatant collected and mixed with 4.2 ml immunoprecipitation buffer (IPB; 1% Triton X-100, 10 mM EDTA, 20 mM Tris-HCl pH 7.6, 150 mM NaCl, 0.17 mM PMSF, 0.17 µg antipain ml⁻¹, 0.17 µg leupeptin ml⁻¹). To reduce non-specific background in subsequent PCR analyses, the lysed chloroplast suspension was cleared by adding 100 µl protein A-Sepharose beads (50% slurry in 10 mM Tris-HCl pH 7.6, 1 mM EDTA, 0.1% BSA) and 10 µl sonicated bacteriophage λ DNA (0.66 µg ml⁻¹). The mixture was incubated on a rotation wheel for 1 h at 4°C. Beads were removed by centrifugation at 2200g for 5 min and the supernatant aliquotted into 1 ml portions. To one tube was added 2 µl rabbit polyclonal antibody to *A. thaliana* TRANSPARENT TESTA GLABRA 1 (TTG1; 37) as a negative control; to a second, 2 µl rabbit polyclonal anti-GFP (ab6556, Abcam plc, <http://www.abcam.com>); a third received no antibody. These three tubes were incubated on a rotation wheel overnight at 4°C. A fourth tube was stored at 4°C for extraction of total DNA later. All of these steps from extraction onwards were performed on the same day to avoid storage and possible degradation of DNA-protein complexes. Following overnight incubation, 40 µl of protein A-Sepharose beads (50% slurry in 10 mM Tris-HCl pH

7.6, 1 mM EDTA, 0.1% BSA) and 1 μ l sonicated λ DNA ($0.66 \mu\text{g ml}^{-1}$) were added to each of the first three tubes which were then incubated on a rotation wheel for 2 h at room temperature. The beads were pelleted at 4500g in a microcentrifuge for 15 s and the supernatant removed and discarded. The protein A-Sepharose beads were washed twice with 400 μ l wash buffer 1 (0.1% SDS, 1% Triton-X 100, 2 mM EDTA, 20 mM Tris-HCl pH 7.6, 150 mM NaCl), once with 400 μ l wash buffer 2 (0.25 M LiCl, 1% Nonidet P-40, 1 mM EDTA, 10 mM Tris-HCl pH 7.6, 24 mM sodium deoxycholate) and twice with 400 μ l TE, with spins of 4500g for 15 s between each wash. Protein-DNA complexes were eluted from the beads by washing the beads three times with 160 μ l elution buffer (1% SDS, 0.1 M NaHCO_3) with a low-speed (4500g) spin between each wash. To 480 μ l of eluate was added 20 μ l 5 M NaCl; 60 μ l 5 M NaCl was also added to the 1 ml portion of chloroplast lysate stored at 4°C. Where a formaldehyde cross-linking step had been included in the immunoprecipitation process, all tubes were incubated in a waterbath for 5–6 h at 65°C to reverse the cross-linking. Two volumes of ethanol were added to each tube and samples were incubated overnight at –20°C to precipitate the protein-DNA complexes. Precipitates were collected by centrifugation, dissolved in 100 μ l TE to which 2 μ l proteinase-K ($18.6 \mu\text{g ml}^{-1}$) was added and incubated for 2 h at 42°C. After addition of 300 μ l TE to each tube, the DNA was extracted with 400 μ l phenol:chloroform:iso-amyl alcohol (25:24:1 by weight) followed by 400 μ l chloroform; care was taken at the final step to collect the same volume of upper layer from each tube to facilitate DNA characterization. Purified DNA was precipitated with two volumes of ethanol in the presence of 5 μ g glycogen overnight at –20°C. The precipitate was collected by centrifugation, washed with 70% cold ethanol and dissolved in 20 μ l TE for analysis by PCR.

Protein immunoblotting

Protein-DNA complexes eluted from washed protein A-Sepharose beads with 1% SDS, 0.1 M NaHCO_3 as described above were used as the source of protein for immunoblotting. Protein-DNA complexes were precipitated with two volumes of ethanol overnight, collected by centrifugation, washed twice in 70% ethanol, air dried for 10 min and then dissolved in 40 μ l 10 mM Tris-HCl pH 7.6. Protein sample buffer (13 μ l of 4 \times concentration: 65 mM Tris-HCl pH 6.8, 10% glycerol, 2% SDS, 5% 2-mercaptoethanol, 0.05% bromophenol blue) was added to each of the samples, which were then boiled for 5 min before being cooled on ice. Total lysate protein (25 μ l) and 35 μ l each of anti-GFP, anti-TTG and no antibody treatments were subjected to SDS-PAGE with a 10% resolving gel and a 5% stacking gel (38). Biotinylated protein markers (#7727, Cell Signalling, <http://www.cellsignal.com>) and 50 ng recombinant GFP (8360-1, Clontech Laboratories Inc., <http://www.clontech.com>) were separated on the same gel. Proteins were transferred to nitrocellulose (Protran BA83, Schleicher & Schuell, <http://www.sigmaldrich.com>)

using a semi-dry blotting apparatus. The membrane was incubated with rabbit polyclonal antibody to GFP (ab290, Abcam plc, <http://www.abcam.com>) at a 1:5000 dilution, followed by biotinylated anti-rabbit Ig antibody (RPN1004, GEHealthcare UK Limited, <http://www.gehealthcare.com>) and streptavidin-biotinylated horseradish peroxidase complex (RPN1051V, GE Healthcare UK Limited, <http://www.gehealthcare.com>) and detected with enhanced chemiluminescence (Western Lightning, Perkin Elmer, <http://www.perkinelmer.com>).

PCR of immunoprecipitated chloroplast DNA

Immunoprecipitated chloroplast DNA was analysed by PCR in a 25 μ l reaction volume containing 1 μ l DNA template, 0.5 u DNA polymerase (BIOTAQ; Boline UK, <http://www.bioline.com>), 2.5 μ l of 10 \times reaction buffer supplied with the enzyme, 2 mM MgCl_2 , 200 μ M each of dATP, dCTP, dGTP, dTTP and 0.3 μ M of each primer. The PCR programme was as follows: 94°C (2 min), 26–28 cycles of 94°C (30 s), 50–60°C (30 s), 72°C (30 s) and 72°C (10 min). PCR fragments were resolved by electrophoresis on a 1.2% agarose gel containing 0.2 μ g ethidium bromide ml^{-1} and visualized with an AlphaImager 1200. Primers used to confirm the presence of *lacO* in immunoprecipitated DNA included a forward primer in the *psbA* 3'-terminal end of *aadA* (5'-GAAATAAGAAAGA GCTATATTCG) and a reverse primer in the *accD* flanking region (5'-TTCAGGGAACTACAACTACAGG). Primers to investigate binding in the *atpBE* region were forward (5'-TCAGCATATCGATTTATGCCTAGC) and reverse (5'-TCTCACAACAACAAGGTCTACTCG) to amplify a fragment of 396 bp. Primers to amplify a 233-bp fragment of 23S rDNA (*rrn23*) were forward (5'-TATCGTGCCACGGTAAACGCTGG) and reverse (5'-CGTAATGATAAACGGCTCGTCTCG). Amplification of a 167-bp fragment from *psbT* was carried out using forward (5'-AAACCACGATCGAATC TATGG) and reverse (5'-GAGGCTCAGTACTTCAAC TG) primers. Amplification of a 3.8 kb fragment from *accD* to *atpBE*, accomplished using the same forward primer for *atpBE* and the reverse *accD* primer as described above, encompassing the *lacO* insertion site, was carried out as described above but with a modified PCR programme incorporating 28 cycles of 94°C (1 min), 55°C (2 min) and 72°C (3 min).

RESULTS

Creation of tobacco lines with plastid-located *lacO* sequences

Chloroplast transformation by biolistics was used to introduce multiple copies of *lacO* into a single site between the *rbcL* and *accD* genes in tobacco chloroplast DNA. Detached leaves of the tobacco cultivar Petite Havana were bombarded with *lacO* plasmids containing either 1 (32 copies) or ~2.5 kb of *lacO* sequences (68 copies) (Figure 1a). Spectinomycin-resistant transplastomic plants regenerated following bombardment with either construct were found to contain a shortened length of *lacO* repeat sequence compared with the transforming

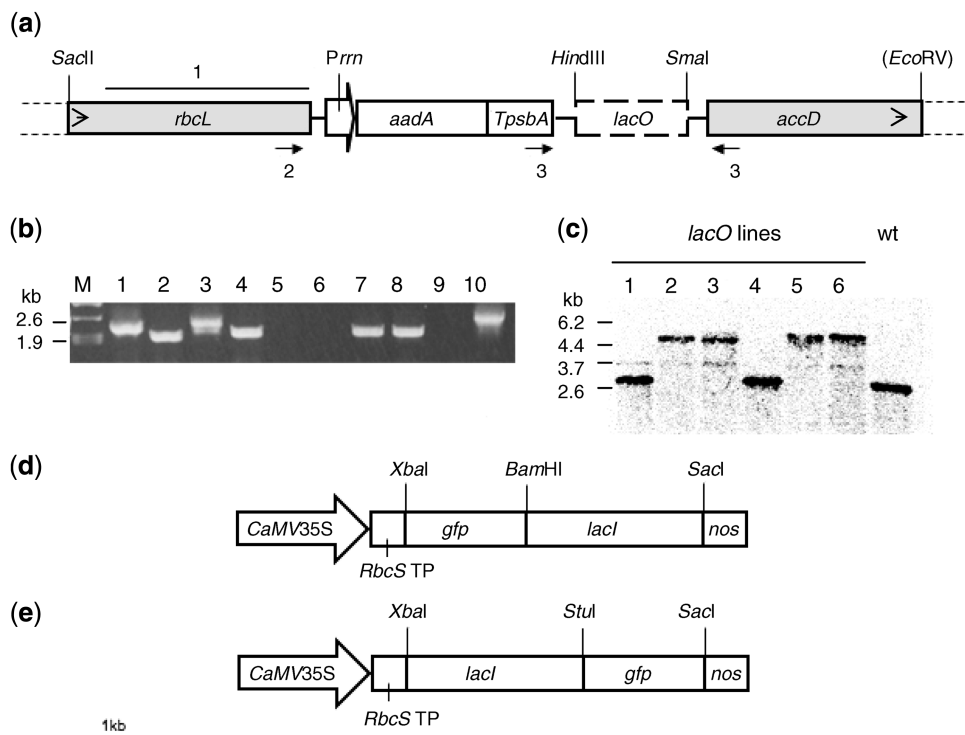


Figure 1. Constructs for plastid and nuclear transformations. **(a)** Construct for plastid transformation. *lacO* DNA (1 or ~2.5 kb; dashed lines) was inserted between the HindIII and SmaI restriction sites into a polylinker in the unique Bsu36I site (31) of pZS197 (30). *Prrm*, plastid *rrn* promoter driving the *aadA* gene conferring resistance to spectinomycin; *TpsbA*, terminator region from plastid *psbA*. Plastid *rbcL* and *accD* sequences are used for recombination into the plastid genome; their direction of transcription is shown by the arrowheads. 1: position of 1.24 kb probe used in Southern DNA analysis. 2: position of the *rbcL* primer used to determine the size of the *lacO* insert in (b); 3: position of the forward and reverse primers used to analyse immunoprecipitated DNA for the presence of *lacO*. **(b)** PCR analysis of leaf DNA from transplastomic *lacO* lines. Lanes 1–4 and 5–8, putative transplastomic lines containing *lacO* constructs with 1 or ~2.5 kb *lacO* DNA, respectively. Lane 9, no-template negative control. Lane 10, positive control, PCR on plasmid containing 1 kb *lacO*. Marker sizes are shown on the left. Primers were used to amplify a region extending from *rbcL* to *accD* and were expected to give band sizes of 2.6 or ~4.0 kb with 1 kb or ~2.5 kb of *lacO*, respectively. **(c)** Southern blot analysis of transplastomic tobacco lines, regenerated following bombardment with a plasmid containing ~2.5 kb *lacO* repeat sequence. Total leaf DNA (0.3 µg) was cut with EcoRV and SacII and probed with a ³²P-labelled 1.24 kb BamHI fragment from *rbcL* [see (a) above]. Lanes 1–6, putative transplastomic lines. WT, 'Petite Havana' wild-type. Band sizes are shown on the left. **(d,e)** Constructs for nuclear transformation containing the *CaMV* 35S promoter and *nos* terminator in pBIN19 (32). **(d)** *gfp-lacI* DNA was inserted between the coding region for the *RbcS* transit peptide and the *nos* terminator using XbaI and SacI restriction sites. **(e)** *lacI-gfp* has been inserted between the coding region for the *RbcS* transit peptide and the *nos* terminator using XbaI and StuI restriction sites.

DNA. PCR analyses of several regenerated lines using primers which flanked the *lacO* insertion site indicated that ~200 bp could be attributed to the inserted *lacO* DNA regardless of the transforming construct (Figure 1b). Transplastomic lines were also subjected to Southern blot analysis. Probing of total leaf DNA digested with EcoRV and SacII with a 1.24 kb BamHI fragment from the plastid *rbcL* gene adjacent to the construct insertion site was expected to give a 2.8 kb band in untransformed plants, and a 5.3 kb band if 2.5 kb of *lacO* DNA had been transferred. The Southern blot detected a band of ~4.4 kb in four of the lines (Figure 1c) confirming the PCR results and indicating that <300 bp of *lacO* DNA was located between the *aadA* selectable marker gene and the *accD* recombination region. Weak hybridization to a band at 3.7 kb was also obtained; this has been observed previously with pZS197-based vectors (29,31) and is probably due to recombination between introduced chloroplast DNA sequences and identical endogenous sequences (39). Recombination frequencies between nearby

repeated sequences in chloroplasts are known to be high (40), and recombination between the repeated *lacO* sequences probably accounts for the substantial reduction in numbers of *lacO* elements in all independent lines tested. This appears to have occurred within 11 weeks of bombardment of the leaves and no further shortening of the *lacO* sequences was observed. Sequencing of PCR products from the transplastomic lines confirmed the presence of three *lacO* repeat sequences of 32 bp each, separated by HaeIII restriction sites and flanked by *EcoRI* sites (Figure 2a), an arrangement similar to the original pAFS plasmid where repeats of eight *lacO* sequences, each separated by a HaeIII restriction site, were themselves separated by *EcoRI* restriction sites (21).

Creation of tobacco lines expressing nuclear-encoded plastid-targeted GFP-LacI and LacI-GFP

Two chimeric genes encoding plastid-targeted N- or C-terminal fusions of LacI to GFP were produced in the binary vector pBIN19 (32), under control of the *CaMV*

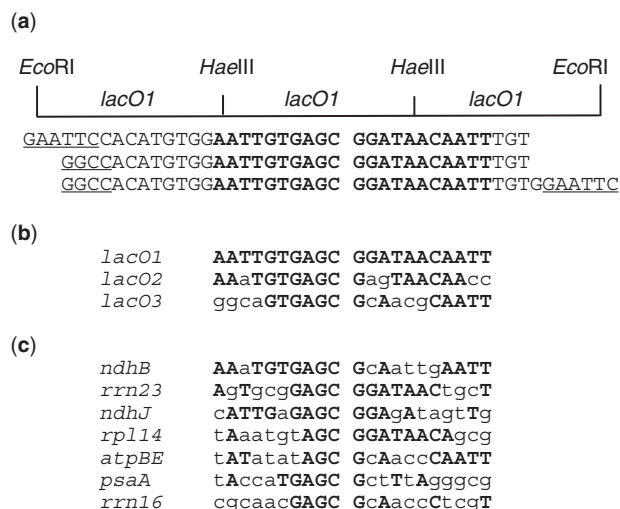


Figure 2. LacI binding sites in *E. coli* and chloroplasts. (a) Arrangement of *lacO* repeats in transplastomic *lacO* lines. *lacO* sequences are separated by HaeIII restriction sites, with an EcoRI restriction site at each end. The sequence of the 118-bp region is given below the diagram. The gap indicates the centre of the dyad symmetry. (b) Core regions of three *lacO* sequences from *E. coli*. Bases identical to *lacO1* are in bold, non-identical bases are lower case. (c) Chloroplast DNA sequences showing similarity to *lacO*. Bases identical to *lacO1* are in bold, non-identical bases are lower case. The locations of the sequences in the tobacco genome (Genbank Z00044) are: *rrn23*, 109075-109095 and 133535-133555; *ndhB*, 98558-98578; *ndhJ*, 51302-51322; *rpl14*, 83504-83524; *atpBE*, 57377-57397; *psaA*, 42101-42121; *rrn16*, 103808-103828 and 138802-138822.

35S promoter (Figure 1d and e) for *Agrobacterium*-mediated transformation of tobacco. GFP-LacI and LacI-GFP were targeted to chloroplasts with the pea RbcS transit peptide. Eleven kanamycin-resistant transgenic lines with the GFP-LacI construct were examined for GFP fluorescence by confocal microscopy. All lines showed a punctate pattern of GFP fluorescence within the plastids (Figure 3a), unlike the uniform GFP fluorescence throughout the stroma found in transplastomic lines expressing soluble GFP (31; Figure 3b). In the highest expressing lines, there was a slight background of GFP fluorescence throughout the chloroplasts, in addition to the punctate pattern. This punctate pattern was similar to the pattern of nucleoids shown in other studies (28). Staining of leaf tissue with the DNA-specific fluorochrome DAPI and examination by epifluorescence microscopy established the co-localization of DAPI and GFP fluorescence (Figure 3c and d), indicating that GFP-LacI was located in plastid DNA-containing nucleoids. A similar punctate pattern of GFP fluorescence within the plastids was observed in lines containing LacI-GFP (Figure 3e). Modification of the C-terminus of the LacI by deleting the last 3–5 amino acid residues has been shown to result in dimeric proteins rather than the wild-type tetramers (41). Attaching GFP to the C-terminus of LacI was therefore likely to interfere with tetramer formation and produce dimeric LacI-GFP fusion protein, which might affect the visualization of GFP binding to *lacO*. However, no differences in the patterns of GFP fluorescence from GFP-LacI and LacI-GFP were observed. Several of the most

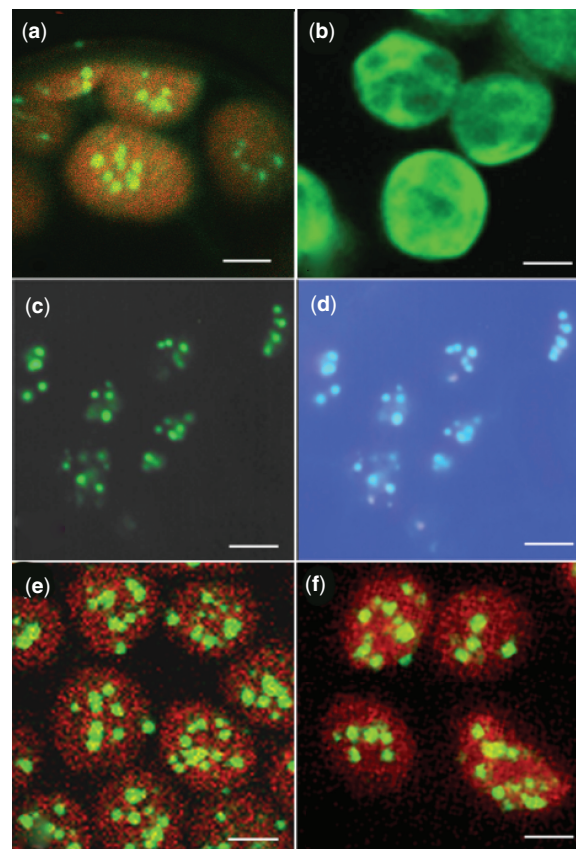


Figure 3. Chloroplasts from tobacco leaf mesophyll cells in water-mounted tissue visualized by confocal or epifluorescence microscopy. (a,b,e,f) Chloroplasts viewed by laser scanning confocal microscopy (TCS-NT, DMRXA light microscope stand, Leica Microsystems Wetzlar GmbH). Images of GFP and chlorophyll fluorescence, using an excitation wavelength of 488 nm, were collected through TRITC and FITC filters, respectively. Images (a), (e) and (f) result from merging chlorophyll and GFP fluorescence. Image (b) shows GFP fluorescence only. (a) GFP-LacI line showing the appearance of plastid DNA as fluorescent nucleoids (bar = 2.8 μ m). (b) *Prrm::gfp* line showing GFP fluorescence distributed throughout the chloroplasts (bar = 2.8 μ m). (c,d) Leaf tissue from a *lacO*/GFP-LacI line stained with DAPI and viewed by epifluorescence microscopy. (c) GFP fluorescence (bar = 2 μ m). (d) DAPI fluorescence of the same cells, merged with GFP fluorescence, showing co-localization of GFP and DAPI-stained DNA (bar = 2 μ m). (e) LacI-GFP line showing the appearance of plastid DNA as fluorescent nucleoids (bar = 2.8 μ m). (f) *lacO*/GFP-LacI line showing fluorescent nucleoids (bar = 2.8 μ m).

strongly expressing LacI-GFP lines showed yellowing of the interveinal regions of the leaves, but this phenotype was not observed with the strongly expressing GFP-LacI lines.

Pollen from a representative homozygous transgenic GFP-LacI line was used to pollinate transplastomic *lacO* lines to combine plastid-located *lacO* and plastid-targeted GFP-LacI in the same plant. The presence of three *lacO* repeats in progeny of the crosses was confirmed by PCR (data not shown) and by DNA sequencing. Examination of the leaves by confocal microscopy indicated a punctate pattern of GFP fluorescence within the chloroplasts (Figure 3f). Progeny from one of these crosses was used for the development of a chloroplast ChIP protocol.

Development of a chloroplast ChIP protocol

In order to develop a chloroplast ChIP protocol, chloroplasts were isolated from leaves of the *lacO*/GFP-LacI plants described above and from three control lines: transplastomic *lacO* plants without GFP-LacI, transgenic GFP-LacI plants without *lacO* and transplastomic *Prrn::gfp* plants which contain high levels of soluble GFP distributed more or less uniformly throughout the stroma with no sign of localization to nucleoids (31). Leaves from 8 to 12 week-old tissue culture-grown plants were routinely used as they contained low levels of starch, which did not interfere with chloroplast extraction, in comparison with plants grown in a growth chamber. A sucrose-based isolation medium was used routinely to aid in stabilization of nucleoid structure within the chloroplasts (26). Fractionation of chloroplasts in a 40/80% Percoll step gradient after extraction resulted in an approximate ratio of 2:1 non-intact:intact chloroplasts. However, under an epifluorescence microscope chloroplasts from both fractions showed bright distinct nucleoids, and therefore unfractionated chloroplast preparations were used in order to maximize recovery of immunoprecipitated material.

Sonication is usually the method of choice to fragment chromatin to protein–DNA complexes containing 300–600 bp DNA in nuclear ChIP methods (1,3). However, sonication of chloroplasts lysed by treatment with 2% Nonidet P-40 was unsuccessful in shearing chloroplast DNA in nucleoids of *lacO*/GFP-LacI plants to small enough fragments to reduce the likelihood of immunoprecipitating long regions that would lower the sensitivity of subsequent PCR analyses. Sonication of the suspension produced by lysing chloroplasts in 2% Nonidet P-40 detergent for 120 s in 30-s bursts reduced the bulk of the DNA to fragments of ~1–3 kb, as estimated by agarose gel electrophoresis. However, it was still possible to amplify regions of 3.8 kb by PCR using a forward primer in the *atpB/E* region 2 kb upstream from the construct insertion site and a reverse primer in the *accD* region adjacent to the 3'-terminus of the inserted DNA, indicating that long fragments of DNA remained. Compact fluorescent nucleoids were also still visible with epifluorescence microscopy following extended sonication of lysed chloroplasts. Digestion with AluI was used by Prikryl *et al.* (9) to fragment maize chloroplast DNA for their ChIP experiments, but digestion with a specific restriction enzyme was thought not to be advisable for generating random fragments of chloroplast DNA. Micrococcal nuclease was therefore tested under various conditions for its ability to digest plastid DNA to smaller fragments (42). A 10-min incubation of lysed chloroplasts with micrococcal nuclease (0.06 u ml^{-1}) at 37°C in Tris–HCl pH 7.6 buffer containing 0.8 mM MgCl₂, 15 mM NaCl and 4 mM CaCl₂, followed by addition of 38 mM EGTA to stop nuclease activity, produced DNA fragments of ~600–1200 bp and it was not possible subsequently to PCR-amplify fragments of 3.8 kb.

The ability of anti-GFP antibodies to immunoprecipitate GFP-LacI complexes from chloroplast extracts was examined by protein immunoblot analysis.

Following micrococcal nuclease treatment, chloroplast extracts were incubated overnight at 4°C with protein A-Sepharose beads and antibodies to GFP, antibodies to TTG1 (a non-chloroplast-located protein) or no antibodies. Proteins eluted from the beads with 1% SDS, 0.1 M NaHCO₃ were separated by SDS-PAGE, blotted onto nitrocellulose and GFP detected with antibodies to GFP and enhanced chemiluminescence. A band of 66 kDa corresponding to the GFP-LacI fusion protein is present in the total chloroplast lysate (Figure 4, lane 4) and in the immunoprecipitate with antibody to GFP (Figure 4 lane 2) but is not present in the immunoprecipitate with antibody to TTG1 or in the absence of antibodies (Figure 4 lanes 1 and 3). The strongly reactive band of ~55 kDa in Figure 4, lanes 1 and 2, is due to the heavy chain of rabbit IgG from the immunoprecipitation incubation cross-reacting with the biotinylated anti-rabbit IgG antibody used in the detection process. It can be concluded that GFP-LacI fusion protein was successfully immunoprecipitated using the antibodies to GFP and protein A-Sepharose.

Formaldehyde is usually used to produce DNA–protein cross-links in nuclear chromatin both *in vivo* and *in vitro* (1,43,44) and, in comparison to other cross-linking reagents, cross-linking can be reversed relatively easily (45). However, formaldehyde cross-linking is not necessary for stabilizing interactions between purified LacI and *lacO*-containing DNA *in vitro* (46). Therefore, the formaldehyde cross-linking step was assessed for its effect on immunoprecipitation of chloroplast DNA–protein complexes. Isolated chloroplasts from *lacO*/GFP-LacI plants were incubated with 1% formaldehyde for 10 min at 22°C, followed by addition of glycine to remove excess formaldehyde and lysis in a buffer containing 2% Nonidet P-40. Following shearing of chloroplast DNA by micrococcal nuclease, complexes containing GFP-LacI were immunoprecipitated with rabbit antibodies to GFP and protein A-Sepharose, eluted from the protein A-Sepharose with SDS and incubated at 65°C for 5–6 h to reverse the cross-links. The extracted

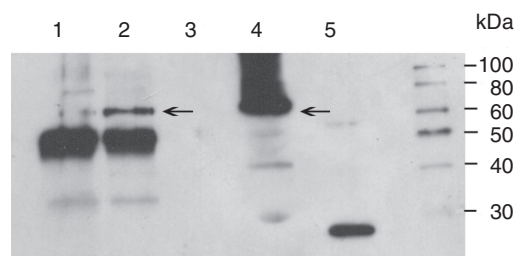


Figure 4. Immunoblot of immunoprecipitated protein obtained by incubation of lysed chloroplast extracts with or without antibody prior to addition of protein-A Sepharose, elution of the protein–DNA complexes from the protein-A Sepharose and subsequent precipitation in ethanol. The precipitates were solubilized in 10 mM Tris–HCl pH 7.6 and 25–35 μ l fractionated by electrophoresis on a SDS-10% polyacrylamide gel, blotted onto nitrocellulose and incubated with rabbit polyclonal anti-GFP. Immunoreactive bands were detected by enhanced chemiluminescence. Lane 1, rabbit anti-*A. thaliana* TTG1; lane 2, rabbit anti-GFP; lane 3, no antibody; lane 4, total soluble protein; lane 5, 50 ng recombinant GFP. Arrows mark the position of the GFP-LacI monomer at 66 kDa. A marker lane is shown to the right.

immunoprecipitated chloroplast DNA was analysed for the presence of *lacO* by PCR using primers that flanked the *lacO* insertion site (Figure 1a) to produce a 409-bp fragment. The *lacO* region was successfully amplified from chloroplast DNA immunoprecipitated by anti-GFP (Figure 5a) but not by anti-TTG1 or no antibody, providing a clear indication that GFP-tagged LacI had bound to the *lacO* sequence in plastid DNA. No amplification of the *lacO* fragment was obtained from the immunoprecipitates of chloroplasts of the three control lines *lacO*, GFP-LacI and *Prrn::gfp* (Figure 5a). Immunoprecipitation of the *lacO* sequence was obtained irrespective of the use of the formaldehyde cross-linking treatment, corroborating the finding that cross-linking was not necessary to stabilize the binding of LacI to *lacO* (46).

The affinity of LacI for *lacO* is reduced 1000-fold in the presence of isopropyl β -D-1-thiogalactopyranoside (IPTG) (47) and, although IPTG can remove LacI from *lacO* binding sites, it does not affect non-specific binding. The addition of IPTG during chloroplast extraction was tested to ascertain whether it would affect binding of LacI to *lacO*. Addition of 20mM IPTG to chloroplasts prior to cross-linking and inclusion in the lysis buffer, immunoprecipitation buffer and at all subsequent stages,

led to a pronounced reduction in the amplified product generated by PCR when primers specific for *lacO* were used (Figure 5b). Even in the presence of excessive amounts of LacI, de-repression by IPTG may not always be complete (48) and, since a high level of GFP-LacI was being expressed from the *CaMV* 35S promoter (Figure 4 and 'Discussion' section), this may be a possible explanation for the small amount of binding of LacI to *lacO* that still seems to be taking place. However, the GFP-LacI fusion protein clearly showed an affinity for *lacO* that could be disrupted by the addition of IPTG, indicating binding of a specific nature.

The appearance of fluorescent GFP foci that co-localized with DNA in plastids of plants transformed with nuclear-encoded GFP-LacI (Figure 3a) suggested that LacI was binding to plastid DNA even in the absence of *lacO*. This might be due to non-specific binding of GFP-LacI to all regions of plastid DNA or to specific binding to endogenous plastid DNA sequences showing similarity to *lacO*. Comparison of the three naturally occurring *lacO* sequences from *E. coli* (Figure 2b) with tobacco plastid DNA identified several locations around the plastome with some sequence similarity to *lacO* (Figure 2c). The *lacO* sequences show pseudo-dyad

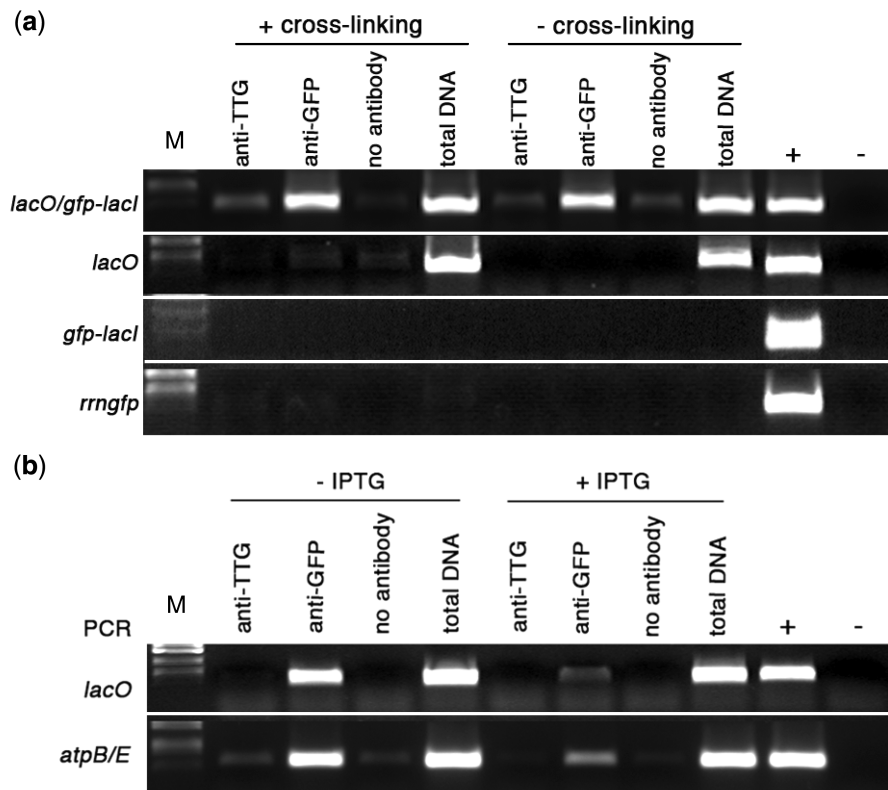


Figure 5. Binding of GFP-LacI to chloroplast-located *lacO* sequences. (a) PCR analysis of immunoprecipitated chloroplast DNA. Immunoprecipitation was carried out with the following treatments: antibody to *A. thaliana* TTG1, antibody to GFP or no antibody. Total DNA was extracted from a fraction of the chloroplast lysate that did not undergo immunoprecipitation. Control reactions for PCR included genomic DNA isolated from a transplastomic *lacO* line (+) and water (-). M, DNA size markers. (a) Binding of GFP-LacI to *lacO*. Primers were used to amplify a 409-bp sequence, which includes plastid-localized *lacO* (marked as position 3 in Figure 1(a)). Experimental lines are listed on the left. Treatments shown in the left half of the panel were carried out following formaldehyde cross-linking, those on the right were not subjected to formaldehyde cross-linking. (b) Effect of IPTG on binding of GFP-LacI to *lacO*. PCR analysis of immunoprecipitated chloroplast DNA from *lacO*/*GFP-LacI* lines, using primers to amplify a 409-bp fragment encompassing *lacO* and a 396-bp fragment from *atpBE* (shown on left side). Treatments shown in the left half of the panel were carried out in the absence of IPTG, those in the right half were carried out in the presence of 20mM IPTG.

symmetry with the central base pairs stabilizing the LacI–*lacO* complex (49,50). We chose to examine binding of GFP-LacI to two regions of plastid DNA (*atpBE* and *rrn23*) containing sequences showing similarity to *lacO*, and to a control region encompassing *psbT*, which was located at least 2 kb away from any region showing similarity to *lacO*. The *lacO* similarity in the *atpBE* promoter region (nucleotides 57372–57392) includes eight consecutive base pairs in the central region identical to *lacO3* (49) suggesting high probability as a binding site for GFP-LacI. The *atpBE* region is located ~3.4 kb from the *lacO* insertion site in the transplastomic *lacO* plants and PCR using *atpBE* and *accD* primers confirmed that the micrococcal nuclease treatment of plastid nucleoids did not produce long fragments of plastid DNA containing both sites. To examine GFP-LacI binding to the *atpBE* region, PCR was performed on immunoprecipitated DNA using primers to amplify a sequence of 396 bp from the *atpB-rbcL* intergenic region. The PCR results (Figure 6a) demonstrate that *atpBE* DNA had been immunoprecipitated from formaldehyde cross-linked treatments of chloroplasts from GFP-LacI lines with or without *lacO*, suggesting that GFP-LacI had bound to plastid DNA in this region. In the absence of formaldehyde, however, there was no amplified DNA band, implying that cross-linking was necessary to stabilize the linkage of weaker protein–DNA complexes during the course of immunoprecipitation. PCR carried out with primers for the *atpBE* region also resulted in a reduced amount of amplified DNA in samples that had been treated with IPTG (Figure 5b), suggesting specific recognition of the *atpBE* site by GFP-LacI.

The other potential GFP-LacI binding site examined occurs within the 23S rDNA sequence where there are 11 consecutive base pairs in the central region identical to *lacO1* (Figure 2c). The PCR results clearly indicate that GFP-LacI also bound to a 233-bp region containing this site. PCR on the anti-GFP-immunoprecipitated DNA gave a positive band in *lacO*/GFP-LacI and GFP-LacI plants, but not in *lacO* or *Prrn::gfp* lines (Figure 6b). The positive results for binding to *lacO*-related sequences in *atpBE* and *rrn23* are in contrast to the results obtained for binding to chloroplast *psbT* region. This region did not appear to contain a *lacO*-related sequence, and the distance to the nearest potential binding site appeared to be ~2 kb. It was not possible to amplify a PCR product of the correct size from any of the immunoprecipitated material (Figure 6c) suggesting that there was little or no binding of GFP-LacI in this region of the genome. This indicates that the location of GFP-LacI in plastid nucleoids is not due to non-specific binding over the complete length of plastid DNA and is likely to be due to specific binding to *lacO*-related sequences. These endogenous binding sites for GFP-LacI appear to be predictable based upon DNA sequence similarity to *lacO*.

DISCUSSION

The binding of a GFP-LacI fusion protein to *lacO* sequences integrated into the chloroplast genome has

been demonstrated by chromatin immunoprecipitation. The binding of GFP-LacI to *lacO* was repressed in the presence of IPTG and its detection by ChIP did not require treatment with formaldehyde, which is commonly used as a reagent to cross-link proteins to DNA. Both these results support the concept that GFP-LacI was binding specifically to *lacO*, as IPTG specifically reduces binding of LacI to *lacO* (47) and formaldehyde cross-linking is not necessary to stabilize *lacO*/LacI binding (46). Binding of GFP-LacI to other sites on the chloroplast genome, as evidenced by the presence of fluorescent nucleoids in the absence of *lacO* (Figure 3), could be detected by ChIP only following cross-linking in the presence of formaldehyde. Two, at least, of these endogenous binding sites appeared to be predictable based on their sequence similarity to naturally occurring *lacO* sequences. The requirement for formaldehyde to stabilize the linkages probably indicates a weaker affinity of the fusion protein for the endogenous sites. However, the affinity of LacI for these endogenous sites would appear to be greater than that of LacI for non-specific binding to DNA. The association constant K_a for LacI binding to *lacO* is $\sim 10^{12} \text{ M}^{-1}$ (51), whereas non-specific binding of LacI to DNA has a K_a of $\sim 10^5 \text{ M}^{-1}$ (52). The absence of any detectable binding of GFP-LacI to the *psbT* region of chloroplast DNA (Figure 6) implies that the ChIP protocol, even in the presence of formaldehyde, does not detect such low-affinity non-specific binding.

The binding of LacI to endogenous binding sites might possibly affect the use of the *lacO*/LacI system to provide an inducible expression system for transgenes in the chloroplast genome. Mühlbauer and Koop (19) demonstrated 20-fold induction of GFP expression from a chimeric *rrn* promoter containing *lacO* sequences on spraying tobacco leaves with IPTG. Binding of LacI to endogenous sites may affect the expression of endogenous chloroplast genes, potentially affecting the growth and development of the plant. No such growth effects were reported (19), suggesting that LacI binding to chloroplast sequences did not have major effects on chloroplast gene expression. In our experiments, yellowing of the interveinal areas of leaves of the most highly expressing LacI-GFP lines was detected, possibly indicating an effect on chloroplast gene expression. However, this was not observed with the most highly expressing GFP-LacI lines, suggesting that the presence of LacI in chloroplasts was not normally detrimental to growth and development.

The amounts of the LacI fusion proteins in chloroplasts are considerably higher than the amount of LacI normally found in *E. coli*, which has been estimated as 5–10 molecules of LacI per cell (48). From western blots of chloroplast extracts with antibodies to GFP, as in Figure 4, it is possible to estimate the ratio of GFP to Rubisco in chloroplasts, assuming that Rubisco accounts for 50% of the chloroplast protein (53). This produces a molar ratio of Rubisco to GFP of 200:1. The number of molecules of Rubisco per chloroplast can be obtained from estimates of mean chloroplast volume and Rubisco concentration. A mean chloroplast volume of $25 \mu\text{m}^3$ can be calculated from the face area of the chloroplasts in Figure 3, assuming a chloroplast thickness of $1 \mu\text{m}$ (54).

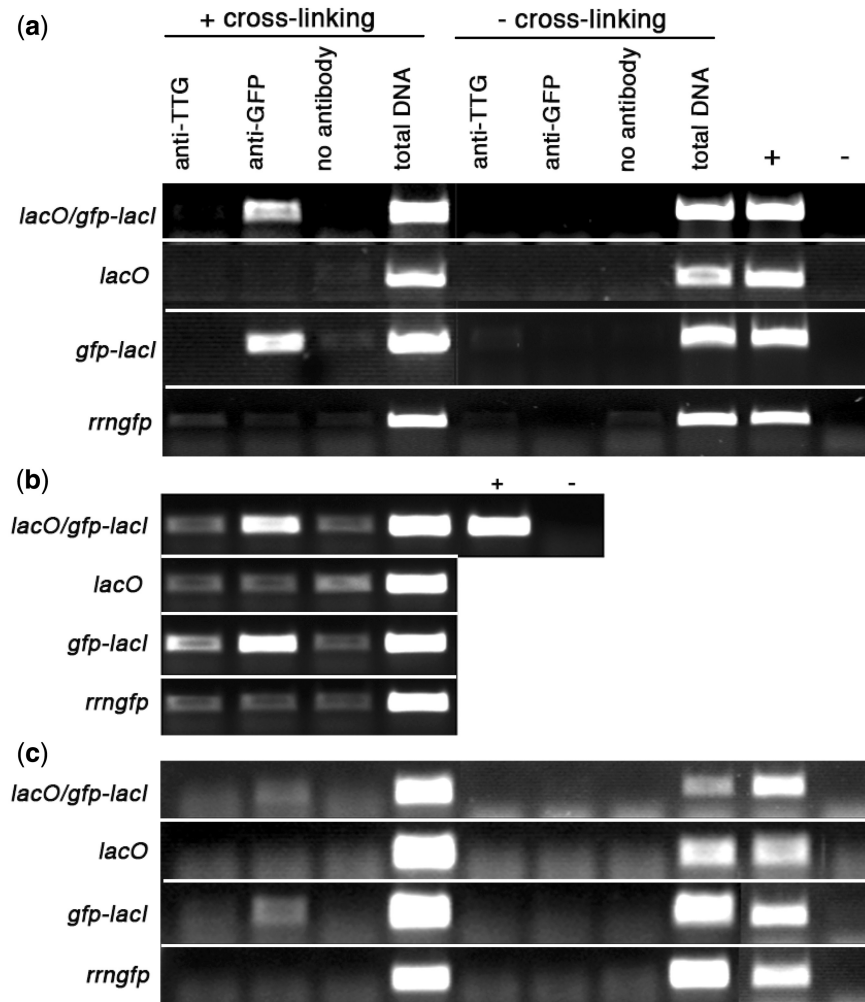


Figure 6. Binding of GFP-LacI to chloroplast sequences. Experimental lines are listed on the left; treatments shown in the left half of the panels were carried out following a formaldehyde cross-linking step, those on the right were not subjected to cross-linking. (a) PCR analysis of immunoprecipitated chloroplast DNA using primers to amplify a 396-bp fragment from plastid *atpB/E*. (b) PCR analysis of formaldehyde cross-linked, immunoprecipitated chloroplast DNA using primers to amplify a 233-bp fragment from plastid 23S rDNA. (c) PCR analysis of immunoprecipitated chloroplast DNA using primers to amplify a 167-bp fragment from plastid *psbT*. Total DNA was extracted from a fraction of the lysate that did not undergo immunoprecipitation. Control reactions for PCR included genomic DNA isolated from a transplastomic *lacO* line (+) and water (-).

Assuming the concentration of Rubisco in the stroma of tobacco chloroplasts is ~ 200 mg/ml, based on the protein concentration of crystals of tobacco Rubisco (55), the number of Rubisco molecules per chloroplast is 6 million. This number is similar to the value of 4.2 million that can be calculated from the Rubisco content (3.6 pg Rubisco per chloroplast) of chloroplasts in the middle region of a developing wheat leaf (56). The estimate of 6 million Rubisco molecules per chloroplast leads to an estimate of 30 000 GFP-LacI molecules per chloroplast. However, these chloroplasts will contain ~ 100 chloroplast DNA molecules, so the ratio of LacI to DNA in chloroplasts is $\sim 300:1$, considerably greater than the 5–10:1 ratio in *E. coli*. This large excess of GFP-LacI is probably responsible for the binding to lower-affinity sites on chloroplast DNA. However, the punctate pattern of GFP fluorescence was still observed in the absence of *lacO* in lower expressing GFP-LacI lines, estimated on the basis of western blotting to have 10-fold

less GFP (data not shown), suggesting that such binding to chloroplast DNA can occur at LacI:DNA ratios not much greater than found in *E. coli*.

The ChIP protocol developed used micrococcal nuclease to fragment the chloroplast genome into suitable small DNA fragments. We decided against the use of a specific restriction enzyme, such as AluI (9), because it would not produce random, overlapping fragments of chloroplast DNA that we believed should maximize the probability of detecting specific protein binding at any site on the chloroplast genome. We failed to identify suitable conditions for the use of sonication, which is the method of choice for fragmenting nuclear and mitochondrial DNA (1,4,7). Neither mitochondria nor chloroplasts contain histones and therefore lack the nucleosome structure of nuclear chromatin. The difference in the susceptibility of the chloroplast and mitochondrial genomes to fragmentation by sonication may therefore be due to differences in the higher order organization of

DNA in the two organelles. Sonication produced ~500-bp fragments of DNA from yeast mitochondria (7), but with chloroplasts it was possible to detect DNA fragments longer than 3 kb following sonication. We therefore used nuclease digestion to ensure that the chloroplast DNA was sheared into small enough fragments to eliminate potentially misleading results of proteins binding at remote sites on long DNA fragments. The micrococcal nuclease digestion protocol was developed to ensure the separation of the *atpBE* region showing similarity to *lacO* and the introduced *lacO* sequences. These sites are ~3.4 kb apart and following digestion it was not possible to amplify long fragments containing both sites. The ChIP experiment should then be able to detect binding at each of the sites independently. By slight modifications of the nuclease digestion protocol it should be possible to detect binding at two even-closer proximal sites by ensuring consistent nuclease cleavage between the two sites.

We believe the ChIP method developed using the introduced *lacO*/LacI system should provide a generic means of identifying specific endogenous protein-binding sites in chloroplast DNA, provided specific antibodies to the DNA-binding protein of interest are available. These antibodies could be raised against the purified protein or synthetic peptides, or against added epitopes, such as HA or MYC tags, or fusion proteins, such as GFP. The use of antibodies against epitope tags or fusion proteins requires the availability of transgenic plants expressing the epitope-tagged or fused DNA-binding protein and this increases the potential risk of aberrant binding to non-physiological target sites by the over-expressed protein. However, the expression of the tagged or fusion protein from its native promoter in a gene-knockout background should minimize this risk. The identification of all binding sites for a particular DNA-binding protein might be achieved by combining the ChIP protocol developed here with a DNA microarray (57). A similar method was used by Prikryl *et al.* (9) to identify fragments of maize chloroplast DNA bound by the WHY1 protein. Although they detected binding to all fragments of AluI-digested maize stromal DNA, the method should be able to detect binding to individual specific regions of the chloroplast genome.

It may be possible to use the chloroplast ChIP protocol to investigate the binding sites of the PEND protein *in organello*. Previous studies have identified potential binding sites *in vitro* by South-western blotting of pea chloroplast fractions (9) or by mobility-shift assay and binding-site selection using the expressed DNA-binding region of PEND (58). The soluble bZIP region of PEND was shown to have a K_a of $\sim 4 \times 10^6 \text{ M}^{-1}$ for a double-stranded oligonucleotide containing two copies of the identified binding-site sequence TAAGAAGT (58). It is difficult to judge if the binding affinity of membrane-associated PEND protein is likely to be similar to that of the soluble bZIP domain, but a higher affinity (higher K_a) is likely to be required to assure success with the ChIP assay. Similar problems may be encountered in trying to use the ChIP assay to detect sigma factor binding at specific sites. Sigma factors provide the specificity for holo-RNA polymerase binding to -35 and

-10 promoter elements, but do not bind DNA in the absence of RNA polymerase (59). The association constant of *E. coli* RNA polymerase holoenzyme containing the σ^{70} sigma factor for canonical promoters is $\sim 10^9 \text{ M}^{-1}$ (60), four orders of magnitude greater than values of $\sim 10^5 \text{ M}^{-1}$ for non-specific binding to DNA (61,62). If the affinity of the chloroplast RNA polymerase holoenzyme containing a specific sigma factor for chloroplast promoter elements is similar to the values of the *E. coli* holoenzyme, the ChIP protocol may be able to detect specific binding, provided the sigma factors are accessible to antibodies and can be immunoprecipitated.

The introduction of the GFP-LacI/*lacO* system into tobacco has made it possible to locate plastid nucleoids throughout plant tissue, in the same way as that demonstrated with the PEND-GFP fusion protein system reported by Terasawa and Sato (28). Plastid nucleoids can be easily visualized in living tissues throughout the plant, including those tissues with non-green plastids that are more difficult to locate using light microscopy. The GFP-LacI/*lacO* plants provide an alternative to the PEND-GFP system (28) that does not require over-expression of an endogenous protein for investigating plastid nucleoid behaviour in various plant organs.

ACKNOWLEDGEMENTS

We would like to thank A. Straight for the gift of plasmids pAFS52 and pAFS59, and T. Kavanagh and J. Jouhet for many helpful discussions during the course of this work.

FUNDING

European Commission as part of FP6 projects PLASTOMICS (grant number LSHG-CT-2003-503238); PHARMA-PLANTA (grant number LSHB-CT-2003-503565). Funding for open access charge: European Commission grant LSHB-CT-2003-503565.

Conflict of interest statement. None declared.

REFERENCES

- Braunstein, M., Rose, A.B., Holmes, S.G., Allis, C.D. and Broach, J.R. (1993) Transcriptional silencing in yeast is associated with reduced nucleosome acetylation. *Genes Dev.*, **7**, 595–604.
- Crane-Robinson, C. and Wolffe, A.P. (1998) Immunological analysis of chromatin: FIS and CHIPS. *Trends Genet.*, **14**, 477–480.
- Chua, Y.L., Brown, A.P.C. and Gray, J.C. (2001) Targeted histone acetylation and altered nucleosome accessibility over short regions of the pea plastocyanin gene. *Plant Cell*, **13**, 599–612.
- Brickwood, S.J., Myers, F.A. and Chandler, S.P. (2002) Methods for the analysis of protein-chromatin interactions. *Mol. Biotechnol.*, **20**, 1–15.
- Kim, T.H. and Ren, B. (2006) Genome-wide analysis of protein-DNA interactions. *Annu. Rev. Genom. Human Genet.*, **7**, 81–102.
- Hall, D.A., Zhu, H., Zhu, X., Royce, T., Gerstein, M. and Snyder, M. (2004) Regulation of gene expression by a metabolic enzyme. *Science*, **306**, 482–484.

7. Kucej,M., Kucejova,B., Subramanian,R., Chen,X.J. and Butow,R.A. (2008) Mitochondrial nucleoids undergo remodelling in response to metabolic cues. *J. Cell Sci.*, **121**, 1861–1868.
8. Rothfuss,O., Fischer,H., Hasegawa,T., Maisel,M., Leitner,P., Meisel,F., Sharma,M., Bornemann,A., Berg,D., Gasser,T. *et al.* (2009) Parkin protects mitochondrial genome integrity and supports mitochondrial DNA repair. *Hum. Mol. Genet.*, **18**, 3832–3850.
9. Prikrýl,J., Watkins,K.P., Frtiso,G., van Wijk,K.J. and Barkan,A. (2008) A member of the Whirly family is a multifunctional RNA- and DNA-binding protein that is essential for chloroplast biogenesis. *Nucleic Acids Res.*, **36**, 5152–5165.
10. Lam,E., Hanley-Bowdoin,L. and Chua,N.-H. (1988) Characterization of a chloroplast sequence-specific DNA binding factor. *J. Biol. Chem.*, **263**, 8288–8293.
11. Baeza,L., Bertrand,A., Mache,R. and Lerbs-Mache,S. (1991) Characterization of a protein binding sequence in the promoter region of the 16S rRNA gene of the spinach chloroplast genome. *Nucleic Acids Res.*, **19**, 3577–3581.
12. Sato,N., Albrieux,C., Joyard,J., Douce,R. and Kuroiwa,T. (1993) Detection and characterization of a plastid envelope DNA binding protein which may anchor plastids nucleoids. *EMBO J.*, **12**, 555–561.
13. Kim,M. and Mullett,J.E. (1995) Identification of a sequence-specific DNA-binding factor required for transcription of the barley chloroplast blue-light responsive *psbD-psbC* promoter. *Plant Cell*, **7**, 1445–1457.
14. Baba,K., Nakano,T., Yamagishu,K. and Yoshida,S. (2001) Involvement of a nuclear-encoded basic helix-loop-helix protein in transcription of the light-responsive promoter of *psbD*. *Plant Physiol.*, **125**, 595–603.
15. Kanamaru,K. and Tanaka,K. (2004) Roles of chloroplast RNA polymerase sigma factors in chloroplast development and stress response in higher plants. *Biosci. Biotechnol. Biochem.*, **68**, 2215–2223.
16. Tsunoyama,Y., Ishizaki,Y., Morikawa,K., Kobori,M., Nakahira,Y., Takeba,G., Toyoshima,Y. and Shiina,T. (2004) Blue light-induced transcription of plastid-encoded *psbD* gene is mediated by a nuclear-encoded transcription initiation factor, AtSig5. *Proc. Natl Acad. Sci. USA*, **101**, 3304–3309.
17. Zghidi,W., Merendino,L., Cottet,A., Mache,R. and Lerbs-Mache,S. (2007) Nucleus-encoded plastid sigma factor SIG3 transcribes specifically the *psbN* gene in plastids. *Nucleic Acids Res.*, **35**, 455–464.
18. Jacob,F. and Monod,J. (1961) Genetic regulatory mechanisms in the synthesis of proteins. *J. Mol. Biol.*, **3**, 318–356.
19. Mühlbauer,S.K. and Koop,H.-U. (2005) External control of transgene expression in tobacco plastids using the bacterial *lac* repressor. *Plant J.*, **43**, 941–946.
20. Robinett,C.C., Straight,A., Li,G., Wilhelm,C., Sudlow,G., Murray,A. and Belmont,A.S. (1996) In vivo localization of DNA sequences and visualization of large-scale chromatin organization using lac operator/repressor recognition. *J. Cell Biol.*, **135**, 1685–1700.
21. Straight,A.F., Belmont,A.S., Robinett,C.C. and Murray,A.W. (1996) GFP tagging of budding yeast chromosomes reveals that protein-protein interactions can mediate sister chromatid cohesion. *Curr. Biol.*, **6**, 1599–1608.
22. Gordon,G.S., Sitnikov,D., Webb,C.D., Telean,A., Straight,A., Losick,R., Murray,A.W. and Wright,A. (1997) Chromosome and low copy plasmid segregation in *E. coli*: visual evidence for distinct mechanisms. *Cell*, **90**, 1113–1121.
23. Kato,N. and Lam,E. (2001) Detection of chromosomes tagged with green fluorescent protein in live *Arabidopsis thaliana* plants. *Genome Biol.*, **2**, research00451–004510.
24. Matzke,A.J.M., van der Winden,J. and Matzke,M. (2003) Tetracycline operator/repressor system to visualize fluorescence-tagged T-DNAs in interphase nuclei of *Arabidopsis*. *Plant Mol. Biol. Rep.*, **21**, 9–19.
25. Kuroiwa,T. (1991) The replication, differentiation, and inheritance of plastids with emphasis on the concept of organelle nuclei. *Int. Rev. Cytol.*, **128**, 1–62.
26. Sato,N., Terasawa,K., Miyajima,K. and Kabeya,Y. (2003) Organization, developmental dynamics, and evolution of plastid nucleoids. *Int. Rev. Cytol.*, **232**, 217–262.
27. James,T.W. and Jope,C.A. (1978) Visualization by fluorescence of chloroplast DNA in higher plants by means of the DNA-specific probe 4'6-diamidino-2-phenylindole. *J. Cell Biol.*, **79**, 623–630.
28. Terasawa,K. and Sato,N. (2005) Visualization of plastid nucleoids in situ using the PEND-GFP fusion protein. *Plant Cell Physiol.*, **46**, 649–660.
29. Birch-Machin,I., Newell,C.A., Hibberd,J.M. and Gray,J.C. (2004) Accumulation of rotavirus VP6 protein in chloroplasts of transplastomic tobacco is limited by protein stability. *Plant Biotech. J.*, **2**, 261–270.
30. Svab,Z. and Maliga,P. (1993) High-frequency plastid transformation in tobacco by selection for a chimeric *aadA* gene. *Proc. Natl Acad. Sci. USA*, **90**, 913–917.
31. Newell,C.A., Birch-Machin,I., Hibberd,J.M. and Gray,J.C. (2003) Expression of green fluorescent protein from bacterial and plastid promoters in tobacco chloroplasts. *Transgenic Res.*, **12**, 631–634.
32. Bevan,M. (1984) Binary *Agrobacterium* vectors for plant transformation. *Nucleic Acids Res.*, **12**, 8711–8721.
33. Farabaugh,P.J. (1978) Sequence of the *lacI* gene. *Nature*, **274**, 765–769.
34. Hoekema,A., Hirsch,P.R., Hooykaas,P.J.J. and Shilperoort,R.A. (1983) A binary plant vector strategy based on separation of *vir*- and *T*-region of the *Agrobacterium tumefaciens* Ti-plasmid. *Nature*, **303**, 179–180.
35. Shen,W.J. and Forde,B.G. (1988) Efficient transformation of *Agrobacterium* spp. by high voltage electroporation. *Nucleic Acids Res.*, **17**, 8385.
36. Horsch,R.B., Fry,J.E., Hoffmann,N.L., Eichholtz,D., Rogers,S.G. and Fraley,R.T. (1985) A simple and general method for transferring genes into plants. *Science*, **227**, 1229–1231.
37. Larkin,J.C., Walker,J.D., Bolognesi-Winfield,A.C., Gray,J.C. and Walker,A.R. (1999) Allele-specific interactions between *ttg* and *gli* during trichome development in *Arabidopsis thaliana*. *Genetics*, **151**, 1591–1604.
38. Laemmli,U.K. (1970) Cleavage of structural proteins during the assembly of the head of the bacteriophage T4. *Nature*, **227**, 680–685.
39. Sinagawa-García,S.R., Tungschat-Huang,T., Paredes-López,O. and Maliga,P. (2009) Next generation synthetic vectors for transformation of the plastid genome of higher plants. *Plant Mol. Biol.*, **70**, 487–498.
40. Iamtham,S. and Day,A. (2000) Removal of antibiotic resistance genes from transgenic tobacco plastids. *Nat. Biotechnol.*, **18**, 1172–1176.
41. Chen,J. and Matthews,K.S. (1992) Deletion of lactose repressor carboxy-terminal domain affects tetramer formation. *J. Biol. Chem.*, **267**, 13843–13850.
42. Simpson,R.T. (1998) Chromatin structure and analysis of mechanisms of activators and repressors. *Methods*, **15**, 283–294.
43. Chaw,Y.F.M., Crane,L.E., Lange,P. and Shapiro,R. (1980) Isolation and identification of cross-links from formaldehyde-treated nucleic acids. *Biochemistry*, **19**, 5525–5531.
44. Chua,Y.L., Channelière,S., Mott,E. and Gray,J.C. (2005) The bromodomain protein GTE6 controls leaf development in *Arabidopsis* by histone acetylation at *ASYMMETRIC LEAVES1*. *Genes Dev.*, **19**, 2245–2254.
45. Jackson,V. (1978) Studies on histone organisation in the nucleosome using formaldehyde as a reversible cross-linking agent. *Cell*, **15**, 945–954.
46. Solomon,M.J. and Varshavsky,A. (1985) Formaldehyde-mediated DNA-protein crosslinking: a probe for *in vivo* chromatin structures. *Proc. Natl Acad. Sci. USA*, **82**, 6470–6474.
47. Riggs,A.D., Newby,R.F. and Bourgeois,S. (1970) Lac repressor-operator interaction. II Effect of galactosides and other ligands. *J. Mol. Biol.*, **51**, 303–314.
48. Gilbert,W. and Müller-Hill,B. (1970) The lactose repressor. In Beckwith,J.R. and Zipser,D. (eds), *The lactose operon*. Cold Spring Harbor Press, NY, pp. 93–109.
49. Bell,C.E. and Lewis,M. (2001) Crystallographic analysis of lac repressor bound to natural operator O1. *J. Mol. Biol.*, **312**, 921–926.

50. Zhang, X. and Gottlieb, P.A. (1995) Modified nucleotides reveal the indirect role of the central base pairs in stabilizing the *lac* repressor-operator complex. *Nucleic Acids Res.*, **23**, 1502–1511.
51. Riggs, A.D., Suzuki, H. and Bourgeois, S. (1970) *lac* repressor-operator interactions: equilibrium studies. *J. Mol. Biol.*, **48**, 67–83.
52. Revzin, A. and von Hippel, P.H. (1977) Direct measurements of association constants for the binding of *Escherichia coli lac* repressor to non-operator DNA. *Biochemistry*, **16**, 4769–4776.
53. Kawashima, N. and Wildman, S.G. (1970) Fraction I protein. *Annu. Rev. Plant Physiol.*, **21**, 325–358.
54. Wildman, S.G., Jope, C.A. and Atchison, B.A. (1980) Light microscopic analysis of the three-dimensional structure of higher plant chloroplasts. Position of starch grains and probable spiral arrangement of stromal lamellae and grana. *Bot. Gaz.*, **141**, 24–36.
55. Baker, T.S., Eisenberg, D., Eiserling, F.A. and Weissman, L. (1975) The structure of form I crystals of D-ribulose-1,5-diphosphate carboxylase. *J. Mol. Biol.*, **91**, 391–399.
56. Dean, C. and Leech, R.M. (1982) Genome expression during normal leaf development. Cellular and chloroplast numbers and DNA, RNA, and protein levels in tissues of different ages within a seven-day-old wheat leaf. *Plant Physiol.*, **69**, 904–910.
57. Chua, Y.L., Mott, E., Brown, A.P.C., MacLean, D. and Gray, J.C. (2004) Microarray analysis of chromatin-immunoprecipitated DNA identifies specific regions of tobacco genes associated with acetylated histones. *Plant J.*, **37**, 789–800.
58. Sato, N. and Ohta, N. (2001) DNA-binding specificity and dimerization of the DNA-binding domain of the PEND protein in the chloroplast envelope membrane. *Nucleic Acids Res.*, **29**, 2244–2250.
59. Helmann, J.D. and Chamberlin, M.J. (1988) Structure and function of bacterial sigma factors. *Annu. Rev. Biochem.*, **57**, 839–872.
60. Strauss, H.S., Burgess, R.R. and Record, M.T. (1980) Binding of *Escherichia coli* ribonucleic acid polymerase holoenzyme to a bacteriophage T7 promoter-containing fragment; evaluation of promoter binding constant as a function of solution conditions. *Biochemistry*, **19**, 3504–3515.
61. Revzin, A. and Woychik, R.P. (1980) Quantitation of the interaction of *Escherichia coli* RNA polymerase holoenzyme to double-stranded DNA using a thermodynamically rigorous centrifugation method. *Biochemistry*, **20**, 250–256.
62. deHaseth, P.L., Lohman, T.M., Burgess, R.R. and Record, M.T. (1978) Nonspecific interaction of *Escherichia coli* RNA polymerase with native and denatured DNA. *Biochemistry*, **17**, 1612–1622.